

Light-induced transformation of vesicles to micelles and vesicle-gels to sols†

Cite this: *Soft Matter*, 2013, 9, 11576

Hyuntaek Oh,^a Vishal Javvaji,^a Nicholas A. Yaraghi,^a Ludmila Abezgauz,^b Dganit Danino^b and Srinivasa R. Raghavan^{*a}

Vesicles are self-assembled nanocontainers that are used for the controlled release of cosmetics, drugs, and proteins. Researchers have been seeking to create photoresponsive vesicles that could enable the triggered release of encapsulated molecules with accurate spatial resolution. While several photoresponsive vesicle formulations have been reported, these systems are rather complex as they rely on special light-sensitive amphiphiles that require synthesis. In this study, we report a new class of photoresponsive vesicles based on two inexpensive and commercially available amphiphiles. Specifically, we employ p-octyloxydiphenyliodonium hexafluoroantimonate (ODPI), a cationic amphiphile that finds use as a photoinitiator, and a common anionic surfactant, sodium dodecylbenzenesulfonate (SDBS). Mixtures of ODPI and SDBS form “catanionic” vesicles at certain molar ratios due to ionic interactions between the cationic and anionic headgroups. When irradiated with ultraviolet (UV) light, ODPI loses its charge and, in turn, the vesicles are converted into micelles due to the loss of ionic interactions. In addition, a mixture of these photoresponsive vesicles and a hydrophobically modified biopolymer gives a photoresponsive vesicle-gel. The vesicle-gel is formed because hydrophobes on the polymer insert into vesicle bilayers and thus induce a three-dimensional network of vesicles connected by polymer chains. Upon UV irradiation, the network is disrupted because of the conversion of vesicles to micelles, with the polymer hydrophobes getting sequestered within the micelles. As a result, the gel is converted to a sol, which manifests as a 40 000-fold light-induced drop in sample viscosity.

Received 13th August 2013
Accepted 25th October 2013

DOI: 10.1039/c3sm52184b

www.rsc.org/softmatter

Introduction

Vesicles are nanoscale containers formed by a variety of amphiphilic molecules, including lipids, surfactants, and block copolymers.^{1–3} They consist of an aqueous core enclosed by a bilayer of the amphiphiles. Vesicles have attracted much interest owing to their potential for the encapsulation and controlled release of substances such as drugs in pharmaceutical applications, flavors and nutrients in foods, fragrances and dyes in cosmetics and textiles, *etc.*^{3–9} Payloads encapsulated in the core of vesicles tend to get released slowly through passive diffusion through the bilayer membrane.^{10,11} However, passive release usually does not deliver a high payload concentration.^{10–12} An alternative is to engineer the vesicles for *active* release; *i.e.*, so that they deliver their entire payload upon activation by an external trigger, such as pH, temperature, ions, enzymes, ultrasound, and light.^{10–15}

Light is an attractive stimulus for triggering release from vesicles due to its high spatial resolution, *i.e.*, it can induce release of encapsulated molecules at a precise location with micron-scale resolution.^{10–12} Accordingly, many researchers have designed light-responsive vesicles, typically using custom-synthesized lipids.^{10–12} For example, vesicles have been created using lipids that contain photocrosslinkable,^{16,17} photoisomerizable,^{18–21} or photocleavable groups.^{22,23} These vesicles exhibit either light-induced disruption of their bilayers or light-activated opening of pores in their bilayers—in both cases, active release of encapsulated payload from the vesicles is triggered by light. However, synthesis of photoresponsive lipids is usually a complex process that requires skills in organic and biochemistry. Thus, the complexity of these previous systems makes them difficult to replicate and scale-up for commercial application. There is a lack of simple and low-cost routes to making photoresponsive vesicles, which is the motivation for the present study.

In our efforts to develop a simple class of photoresponsive vesicles, we focus on vesicles formed by single-tailed amphiphiles (surfactants) due to their simplicity and ease of preparation.^{24–27} It is well-known that a mixture of cationic and anionic surfactants can spontaneously self-assemble into nanoscale unilamellar vesicles in water.²⁴ These “catanionic”

^aDepartment of Chemical and Biomolecular Engineering, University of Maryland, College Park, MD 20742-2111, USA

^bDepartment of Biotechnology and Food Engineering, Technion – Israel Institute of Technology, Haifa, 32000, Israel. E-mail: sraghava@umd.edu

† Electronic supplementary information (ESI) available. See DOI: 10.1039/c3sm52184b

vesicles are indefinitely stable and can be formed by simple mixing (*i.e.*, there is no need for extrusion or sonication).^{24,25} The vesicles can encapsulate payloads in their aqueous core much like conventional lipid vesicles.^{26,27} How can these vesicles be made photoresponsive? One straightforward possibility is to combine a photoresponsive surfactant with a conventional surfactant of opposite charge. Indeed, this approach has been tried and does give rise to photoresponsive vesicles, as demonstrated by several authors using azobenzene-modified cationic surfactants.^{28–31} However, chemical synthesis is still necessary to incorporate azobenzene or similar groups into the surfactant molecules, and that is something we wish to avoid.

Here, we present a simple design for photoresponsive vesicles that uses only molecules that are commercially available and relatively inexpensive. The impetus for our study was the observation that alkyl-substituted diaryliodonium salts, which are frequently used as cationic photoinitiators,^{32,33} have an amphiphilic nature. In particular, we have worked with the molecule, *p*-octyloxydiphenyliodonium hexafluoroantimonate (ODPI),^{34,35} and we confirm that this molecule acts as a cationic surfactant. Accordingly, we combine ODPI with the common anionic surfactant sodium dodecylbenzenesulfonate (SDBS), and as expected, these mixtures form unilamellar catanionic vesicles at certain compositions. The chemical structures of ODPI and SDBS are shown in Fig. 1a and b, respectively, and a schematic of the vesicles is shown in Fig. 1c. It is further known that molecules such as ODPI lose their cationic charge by photodissociation

when irradiated with ultraviolet (UV) light.^{32,33} Thus, when ODPI–SDBS vesicles are exposed to UV light, the loss of charge on ODPI results in a transition from vesicles to spherical micelles (Fig. 1c). Such a transition will be accompanied by complete release of the internal payload within the vesicles into the surrounding aqueous solution.^{26,27}

As an additional potential application, we demonstrate that these photoresponsive vesicles can be used to design a new class of photorheological (PR) fluids whose rheology can be tuned by light irradiation.^{36,37} By combining the ODPI–SDBS photoresponsive vesicles with an associating polymer, *viz.* hydrophobically-modified alginate (hm-alginate), we demonstrate a photoresponsive vesicle-gel. A vesicle-gel is a volume-filling network of vesicles bridged by polymer chains, and it is formed because the hydrophobes on hm-alginate chains insert into the hydrophobic bilayers of vesicles.^{38–41} Upon UV irradiation, the vesicles in the gel are transformed into micelles, thereby disrupting the original network and causing a gel-to-sol transition.

Results and discussion

ODPI–SDBS vesicles

The photoresponsive vesicles described here are created by combining aqueous solutions of the cationic photoinitiator ODPI and the anionic surfactant SDBS. ODPI is an alkyl substituted diphenyliodonium salt (Fig. 1a) that is widely used as a photoinitiator for UV and near-infrared (NIR) polymerization.^{34,35} We note that ODPI has an octyl tail and a cationic head group. This suggests that ODPI is amphiphilic and that it could serve as a cationic surfactant. Surface tensiometry confirms this point. As shown in Fig. S1 (ESI[†]), the addition of ODPI to water decreases the surface tension up to a plateau value of 32.5 mN m^{-1} . From the inflection point of the surface tension plot,² we estimate its critical micelle concentration (CMC) to be 1.3 mM. Incidentally, the CMC of the anionic surfactant SDBS is reported to be 1.4 mM.⁴² Thus, ODPI and SDBS are surfactants with similar CMC values, but with opposite charges.

We proceeded to examine the phase behavior of ODPI–SDBS mixtures at a total surfactant concentration of 1 wt%. Samples with various weight ratios of ODPI to SDBS were prepared in 50 mM phosphate buffer solutions. We used a buffer rather than deionized water to ensure that the pH remained stable with time. On their own, both ODPI and SDBS form clear solutions in buffer. When the two solutions are mixed, samples at ODPI : SDBS ratios between 2 : 8 and 4 : 6 are homogeneous and cloudy with a bluish tint, which is indicative of vesicle solutions (Fig. 2).⁴³ Samples at ODPI : SDBS ratios of 5 : 5 and 6 : 4 reveal some visible solid precipitation, while samples with higher ODPI content (ODPI : SDBS from 7 : 3 to 9 : 1) separate into co-existing liquid phases. The above phase behavior of ODPI–SDBS mixtures is reminiscent of other cationic/anionic surfactant mixtures. In particular, mixtures of cationic surfactants like cetyl trimethyl-ammonium tosylate (CTAT) with SDBS also give rise to vesicles at ratios similar to those in Fig. 2.^{24,25} For a fixed weight ratio of ODPI : SDBS = 3 : 7 (corresponding to

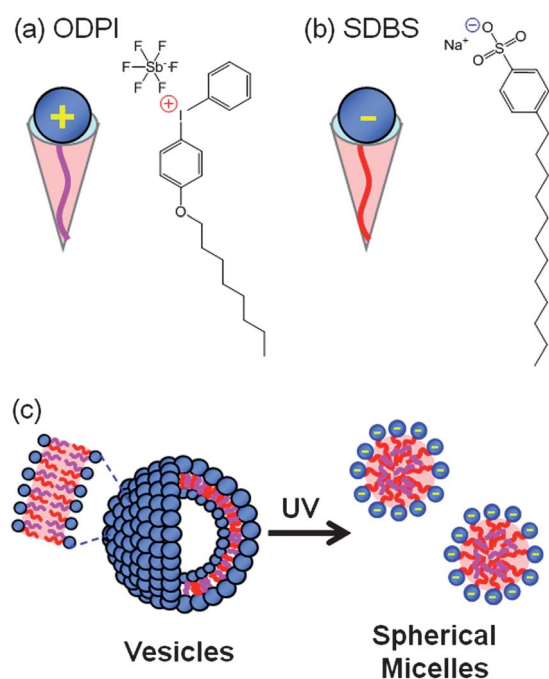


Fig. 1 Components of our photoresponsive vesicles: (a) the cationic amphiphile ODPI and (b) the anionic surfactant SDBS. Vesicles formed by combining ODPI and SDBS are transformed by UV light into spherical micelles. This is shown schematically in (c).

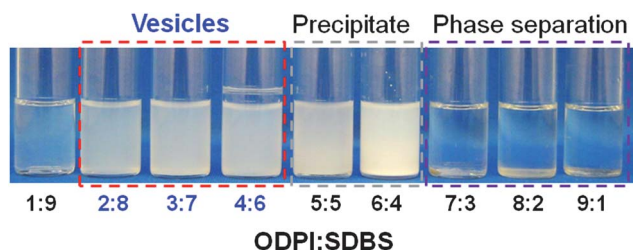


Fig. 2 Phase behavior of ODPI-SDBS mixtures at a fixed total concentration of 1 wt% in aqueous buffer. Samples at ODPI : SDBS weight ratios between 2 : 8 and 4 : 6 show the presence of vesicles. The bluish tinge of these samples reflects light scattering from vesicles. At higher ODPI content (5 : 5 and 6 : 4), samples reveal a whitish precipitate. At even higher ODPI content (7 : 3 to 9 : 1) the samples separate into two liquid phases.

a molar ratio of 1 : 4.3), homogeneous vesicle-bearing samples are found over a window of total surfactant concentration from about 0.1 to 4 wt%. Above 4 wt%, the mixtures become inhomogeneous and show a solid precipitate.

The vesicle-containing ODPI-SDBS mixtures were analyzed further. The samples remained homogeneous and unchanged for several weeks when stored in the dark at room temperature. The size of structures in solution was measured by dynamic light scattering (DLS). For a sample of 1 wt% total surfactant at a ratio of ODPI : SDBS = 3 : 7, the hydrodynamic diameter D_h measured by DLS was 110 nm. This size was maintained over a period of weeks, *i.e.*, there was no aggregation or coalescence of the vesicles. While DLS and visual observations are strongly suggestive of vesicles, we resorted to the technique of cryo-transmission electron microscopy (cryo-TEM) for definitive evidence in this regard.^{44–46} Fig. 3a shows a representative cryo-TEM image of the above ODPI-SDBS sample. The image indeed confirms the presence of unilamellar vesicles in the sample, which are each seen to have a distinct dark shell (bilayer) enveloping their aqueous core.⁴⁶ The vesicles range from 30 to 120 nm in diameter, which is broadly consistent with the DLS measurement.

Vesicle to micelle transition induced by light

We now discuss the effect of UV irradiation on the 1 wt% ODPI : SDBS = 3 : 7 sample. As shown in Photo 1 of Fig. 3, this vesicular sample is initially turbid with a bluish tint and the D_h from DLS was 110 nm. Upon UV irradiation, the sample gradually loses its turbidity and becomes transparent and yellowish (Photo 2 in Fig. 3). The loss of turbidity indicates a structural transformation to much smaller structures.⁴³ After 1 h of UV irradiation, the D_h from DLS was found to be 8.2 nm. Such a low value of D_h suggests that the vesicles must have been converted into micelles.⁴³ To confirm this aspect, we again resorted to cryo-TEM. A representative cryo-TEM image of the irradiated sample is shown in Fig. 3b and it indeed reveals the presence of spherical micelles, which appear as black spots in the image.⁴⁶ The size of these micelles is about 3 to 5 nm, which is much smaller than the vesicles. Note the absence of any larger entities in the photograph as well as the cryo-TEM image, which implies that the irradiated sample is a homogeneous, single-phase micellar solution.

The UV-induced vesicle-to-micelle transition in ODPI-SDBS mixtures is readily explained based on the photochemistry of ODPI. Diphenyliodonium salts like ODPI are known to undergo photodissociation, whereby the molecule loses its positive charge and generates a proton (indeed, ODPI is an example of a “photoacid generator”).^{32,33} In the present case, the protons are not responsible for the structural transition. All samples were prepared in buffer solution and the measured pH of the sample before and after UV irradiation was almost the same at around 7.5. Also, ODPI-SDBS vesicles are stable and display identical sizes over a wide range of pH (3–12). Rather than the protons, it is the loss of positive charge on ODPI that explains the UV-induced transition, as depicted in Fig. 4. Once ODPI dissociates, the molecule becomes nonionic and hydrophobic, which is shown as pink tails (without a head) in Fig. 4. In contrast, the initial ODPI is a surfactant, shown as a pink tail with a blue cationic head. This difference in molecular geometry impacts the packing of the molecules within self-assembled structures.

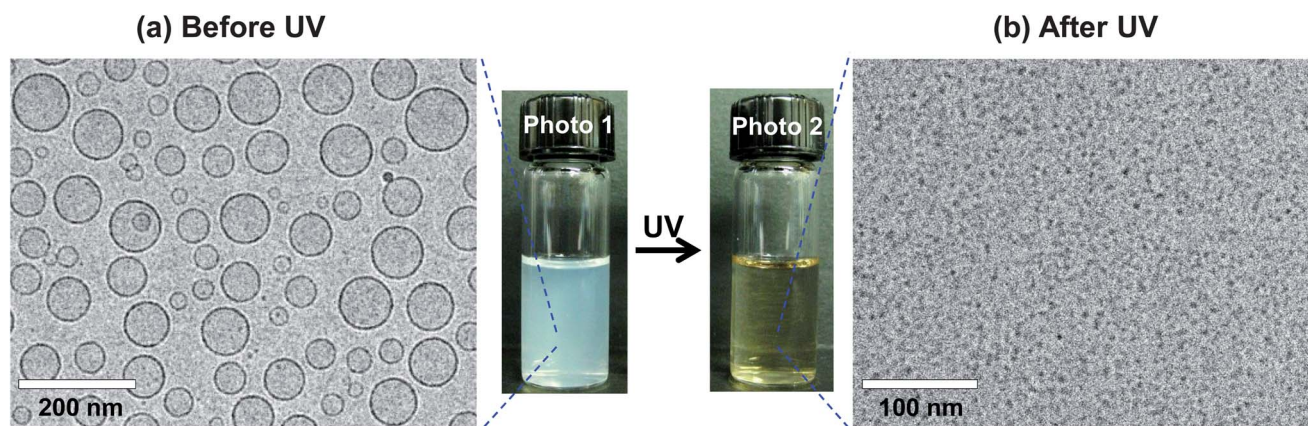


Fig. 3 Vesicle to micelle transition induced by UV light, as shown by visual observations and cryo-TEM images. The sample is a 1 wt% mixture of ODPI : SDBS = 3 : 7. (a) Initially (before UV exposure), the sample shows a bluish tinge and high turbidity (Photo 1). Under cryo-TEM, numerous unilamellar vesicles with diameters between 30 and 120 nm are seen. (b) After 1 h of UV irradiation, the sample is transformed into a transparent, yellowish solution that weakly scatters light (Photo 2). Under cryo-TEM, spherical micelles with a size around 3–5 nm are seen.

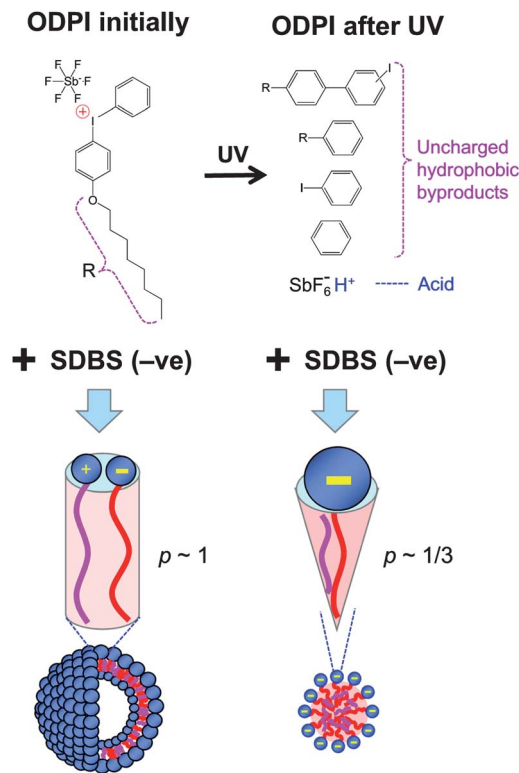


Fig. 4 Mechanism for the UV-induced conversion of ODPI-SDBS vesicles to micelles. Initially, ODPI is cationic and it pairs with the anionic SDBS, giving a cylindrical geometry ($p \sim 1$) that leads to vesicles. UV irradiation transforms ODPI into uncharged byproducts (pink tails). In this case, the lack of cationic species to pair with the anionic heads of SDBS implies a net cone shape ($p \sim 1/3$), in turn leading to spherical micelles. The pink tails are embedded in the hydrophobic cores of these micelles.

It is useful to invoke the concept of the critical packing parameter in this context.^{1,2} This parameter $p = a_{\text{tail}}/a_{\text{head}}$, *i.e.*, it is a ratio of the average area of the tail region (a_{tail}) to the average area of the head region (a_{head}). The head area (a_{head}) includes the influence of electrostatic charge, *i.e.*, when the head is charged, a_{head} will be large. Initially, when ODPI and SDBS are mixed, the cationic heads of ODPI will bind with the anionic heads of SDBS, creating ion-paired complexes.^{24,25} These complexes will have comparable a_{tail} and a_{head} and will assume the overall shape of a cylinder ($p \sim 1$), as shown in Fig. 4. This geometry favors the formation of bilayers and in turn vesicles.^{1,2} (Note that the vesicles still have an excess of one surfactant, which in turn imparts a net charge to the bilayer that may help to stabilize the vesicles.) Upon UV irradiation, the loss of charge on ODPI will leave only the anionic SDBS with a net charge on its head, and this will mean a large a_{head} . Such a molecule will take on a cone shape ($p \sim 1/3$), *i.e.*, its head area will far exceed its tail area (Fig. 4). This geometry favors the formation of spherical micelles.^{1,2} Note that the hydrophobic byproducts of ODPI photodissociation are expected to get sequestered in the cores of SDBS micelles. That is why the sample remains homogeneous after UV irradiation.

In closing this section, we reiterate that our photoresponsive vesicles are one of the simplest classes of light-sensitive

nanocontainers. The mixture of ODPI and SDBS, two well-known commercially available compounds, results in spontaneous assembly into unilamellar vesicles, and light causes a phase transition of these vesicles to spherical micelles. A noteworthy aspect here is that both the initial and the irradiated states are stable, homogeneous and well-defined. This is in contrast to many previous light-responsive vesicle systems, where light-induced complete disruption of the bilayer causes the vesicles to aggregate or transform into an undefined precipitate.^{22,28,30}

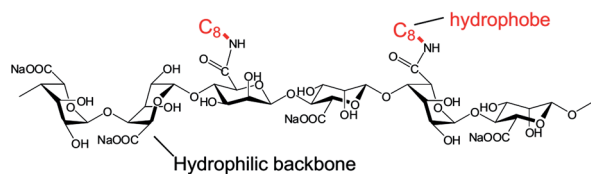
Vesicle-gels using ODPI-SDBS vesicles and hm-alginate

Next, in addition to light-triggered disruption of nanocontainers, we investigated the use of our photoresponsive vesicles to design photorheological (PR) fluids, *i.e.*, fluids that undergo a significant change in their rheological properties upon exposure to light.^{36,37} For this, we created a “vesicle-gel” using ODPI-SDBS vesicles. A vesicle-gel, as demonstrated by us and others, is obtained by adding an associating polymer to a solution of vesicles.^{38–41} Associating polymers are those with a hydrophilic backbone and hydrophobes that are either attached at the chain ends or along the chain backbone.⁴⁷ When added to vesicles, the hydrophobes on the polymer chains get embedded in vesicle bilayers, thus bridging the vesicles into a three-dimensional network (see Fig. 7a).⁴⁰ The sample then becomes either gel-like (highly viscoelastic, with a long, but finite relaxation time) or a true elastic gel with an infinite relaxation time.^{38–41}

To gel the ODPI-SDBS vesicles, we synthesized a hydrophobic derivative of the biopolymer alginate using established procedures (see Experimental section for details).^{48–50} The resulting hydrophobically modified alginate (hm-alginate) bears octyl (C_8) groups along its backbone, as shown in Fig. 5a. The degree of hydrophobic modification was determined to be 23% by NMR (see Fig. S2, ESI†). Note that hm-alginate has an anionic character due to the residual carboxylate groups on the polymer. The vesicles at a ratio of ODPI : SDBS = 3 : 7 are also anionic (since the anionic surfactant SDBS is in molar excess).

Fig. 5b describes vesicle-gel formation upon mixing non-viscous solutions of the above ODPI-SDBS vesicles and hm-alginate. As seen in Plot 1, a 3 wt% solution of the vesicles is a Newtonian fluid with a low viscosity around 2 mPa s. A 1 wt% solution of hm-alginate also shows a viscous response,⁵¹ as indicated by its dynamic rheological data in Plot 2. That is, the elastic (G') and viscous (G'') moduli are strong functions of frequency ω , with $G'' > G'$ over the frequency range. When 1 wt% hm-alginate is combined with 3 wt% vesicles, the mixture is instantly turned into a gel that holds its weight in the inverted vial (Photo 3). Note that the vesicle-gel is bluish and cloudy, similar to the vesicle sample (Photo 1). The gel shows a predominantly elastic response in dynamic rheology (Plot 3): *i.e.*, $G' > G''$ over the ω range, and with both moduli showing a weak dependence on ω . Such a response is indicative of a gel-like material comprising a transient physical network.⁵¹ The same sample under steady-shear rheology shows a zero-shear viscosity η_0 around 400 Pa s (Fig. 6a). It also exhibits weak shear-thickening beyond the Newtonian regime, which is often

(a) hm-alginate (associating polymer)



(b) Vesicle-gel formation

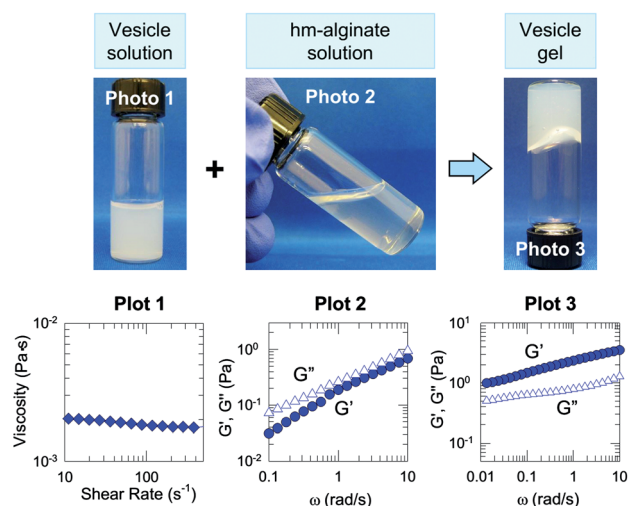


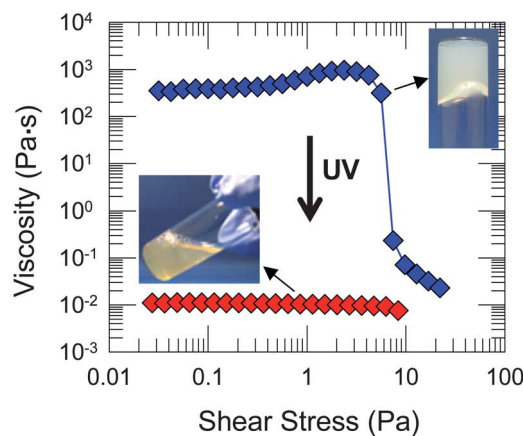
Fig. 5 Vesicle gel formation by combining hm-alginate and ODPI-SDBS vesicles. (a) Molecular structure of hm-alginate. (b) Photographs and rheological data demonstrating the formation of a vesicle gel. A sample of 3 wt% ODPI : SDBS = 3 : 7 vesicles is initially a low-viscosity fluid (Photo 1) and shows Newtonian behavior in steady-shear rheology (Plot 1). This is combined with a 1 wt% solution of hm-alginate (Photo 2), which is moderately viscous, as shown by data from dynamic rheology (Plot 2). The mixture results in a vesicle gel that holds its weight in the inverted vial (Photo 3) and shows an elastic response in dynamic rheology (Plot 3). In plots 2 and 3, the elastic modulus G' (filled circles) and the viscous modulus G'' (unfilled triangles) are depicted as functions of the angular frequency ω .

observed in solutions of associating polymers.⁴⁷ When the shear stress exceeds 5 Pa, a steep drop in viscosity is observed. This is akin to a yield stress, *i.e.*, the sample hardly flows at stresses below this value, as seen in Photo 3.^{47,51}

Vesicle-gel to sol transition induced by light

Next, we investigated the effect of UV irradiation on the above vesicle-gel. Visual inspection revealed that the gel was turned into a thin, freely-flowing liquid (sol) when exposed to UV light. A photograph of the UV-irradiated sample is shown in the inset to Fig. 6a. The sample has the yellowish tinge previously observed in Photo 2 of Fig. 3; note the contrast in both color and flow properties with the initial vesicle-gel sample. These visual observations are corroborated by data from steady-shear and dynamic rheology. The steady-shear data (Fig. 6a) indicate that the gel ($\eta_0 \approx 400$ Pa s) is converted to a Newtonian sol with a viscosity of 10 mPa s (*i.e.*, a reduction by a factor of 40 000). The data from dynamic rheology (Fig. 6b) confirm the viscous nature of the irradiated sample, *i.e.*, $G'' > G'$ with the moduli being

(a) Steady rheology



(b) Dynamic rheology

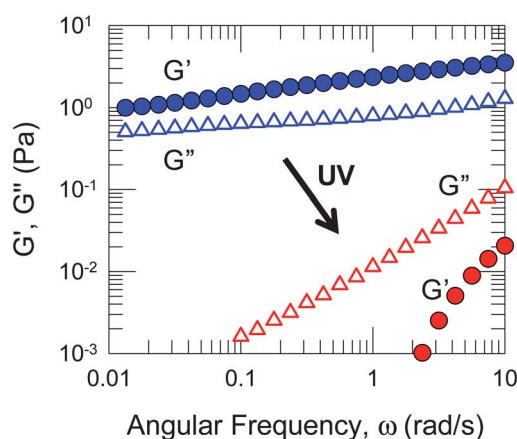


Fig. 6 Gel-to-sol transition of the photoresponsive vesicle gel upon UV irradiation. Data from steady-shear rheology (a) and dynamic rheology (b) are shown for a vesicle gel obtained by mixing a 3 wt% ODPI : SDBS = 3 : 7 vesicles and a 1 wt% hm-alginate solution. In (a) the apparent viscosity is shown as a function of shear stress. In (b), the elastic modulus G' (filled circles) and the viscous modulus G'' (unfilled triangles) are plotted against the angular frequency ω . Before UV irradiation (blue symbols), both sets of data indicate gel-like behavior of the sample. After UV irradiation, the sample is reduced to a thin fluid that exhibits purely viscous, Newtonian behavior. This is corroborated by the photos shown in the inset of (a).

strong functions of frequency. This is in contrast to the elastic gel-like response of the sample prior to irradiation.

We attribute the light-induced gel-to-sol transition of the above sample to the light-induced transformation of ODPI-SDBS vesicles to micelles. The scenario is depicted in Fig. 7. Initially, when the vesicles are mixed with hm-alginate, a vesicle-gel is formed as shown in Fig. 7a. Here, the hydrophobes on the polymer chains are inserted into vesicle bilayers and the vesicles thus act as multi-functional crosslinks in a network structure.⁴⁰ As demonstrated by dynamic rheology, the bonds in this network relax very slowly, and the sample thus exhibits gel-like behavior with a yield stress.⁴⁷ Upon UV irradiation, a transition from vesicles to spherical micelles occurs. The hydrophobes are now expected to be embedded ("solubilized") in the spherical micelles, as shown in Fig. 7b. Because micelles

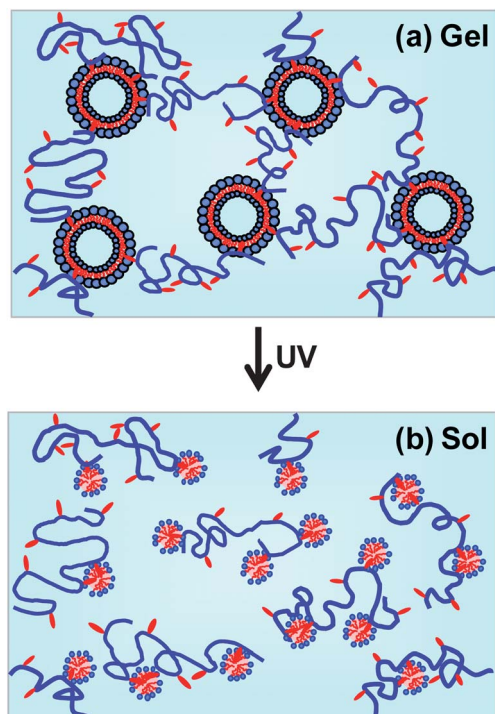


Fig. 7 Mechanism for the UV-induced gel-to-sol transition. Initially, when ODPI-SDBS vesicles and hm-alginate are combined, a vesicle gel is obtained, as shown in (a). Here, the hm-alginate chains are depicted with a blue backbone and red hydrophobic pendant groups. The hydrophobes embed in the bilayers of vesicles, also shown in red, *via* hydrophobic interactions. The result is that the vesicles become connected by the polymer chains into a network, which explains the gel-like behavior. Upon UV irradiation, the vesicles are transformed into spherical micelles (b). These micelles enclose and sequester the hydrophobes on the polymer chains. As a result, the crosslinks in the network are eliminated and the sample is converted to a sol.

are much smaller than vesicles, they will typically enclose individual hydrophobes, but will be isolated from other polymer chains.⁴⁷ Note also that spherical micelles are dynamic structures that break and re-form frequently due to rapid surfactant exchange,⁵² whereas vesicles are relatively static structures due to a much slower rate of surfactant exchange.² In other words, micelles cannot serve as crosslinks in the same way as vesicles.⁴⁰ All in all, the transition from vesicles to micelles eliminates the crosslinks that held the network in place. This explains the gel-to-sol transition and thus the PR effect.

We have considered an alternate possibility for the UV-induced PR effect, which is that reflects the scission of hm-alginate chains due to radicals generated by photodissociation of ODPI.^{32,33} To test this, we solubilized ODPI in micelles of the nonionic surfactant Triton X100 and added it to solutions of alginate and hm-alginate. No changes in viscosity were observed in these solutions upon UV irradiation. (Note that if ODPI was directly mixed with alginate, it formed a precipitate due to the opposite charges on the two moieties.) Thus, the PR changes cannot be attributed to the effect of radicals. This is probably because the generated radicals are expected to be hydrophobic, and would get buried in the interior of micelles *i.e.*, they would not directly interact with the polymer chains or with the surfactant head groups.

We also studied the PR response for different concentrations of hm-alginate and the vesicles. First, we fixed the vesicles at 2 wt% and varied the hm-alginate concentration. Data are shown in Fig. S3 (ESI[†]) for the low-shear viscosity η_0 before and after UV irradiation. At low concentrations of hm-alginate (~ 0.5 wt%), the sample is not gel-like because there are too few polymer chains to connect the vesicles into a network.⁴⁰ On the other hand, at high concentrations of hm-alginate (>1.5 wt%), there is very little difference in η_0 before and after irradiation. This is because at high concentrations, hm-alginate can form a gel-like network by itself through associations between its hydrophobes, *i.e.*, even in the absence of vesicles.^{48,49} Next, we fixed the hm-alginate at 1 wt% and varied the vesicle content. Below 1 wt% vesicles, the samples are again not gels because there are insufficient vesicles to connect the polymer chains into a network.⁴⁰ Gels do form for >1 wt% vesicles, and the viscosity η_0 and yield stress of the gels increase with vesicle concentration (Fig. S4, ESI[†]). After UV irradiation, these vesicle-gels become non-viscous solutions regardless of the vesicle concentration. Thus, in order to maximize the PR effect, it is better to use a moderate concentration of hm-alginate (~ 1 wt%) and a high concentration of ODPI-SDBS vesicles.

An attractive feature of these vesicle-gel-based PR fluids is that vesicles, *i.e.*, nanocontainers, are present in the gel state whereas these containers are disrupted and converted to micelles in the sol state. Thus the light-induced gel-to-sol transition can be combined with light-triggered release of payloads encapsulated in the vesicles. Consequently, the current fluids may be envisioned as a type of photoresponsive delivery system (*e.g.*, an injectable gel) for drug delivery or controlled release applications.⁴¹

Conclusions

We have described a simple class of photoresponsive vesicles that transform into spherical micelles upon UV irradiation. These are prepared by mixing two inexpensive and commercially available surfactants, *viz.* the cationic ODPI and the anionic SDBS. The oppositely charged head groups of ODPI and SDBS bind to each other, resulting in cylinder-shaped pairs of molecules, which spontaneously assemble into vesicles. When these vesicles are irradiated by UV light, ODPI molecules lose their positive charge and become hydrophobic. SDBS head groups then no longer have a binding partner and so the molecular geometry assumes a cone shape, which explains the transition to spherical micelles. Using the above vesicles, we have also demonstrated a photoresponsive vesicle-gel that is converted to a sol by UV irradiation. The gel is created by combining the associating biopolymer hm-alginate with the ODPI-SDBS vesicles. hm-Alginate chains bind to the vesicles *via* hydrophobic interactions between the hydrophobes and vesicle bilayers; in turn, the vesicles become connected by polymer chains into a network. Upon UV irradiation, the vesicles are converted into micelles, and the resulting micelles envelop the hydrophobes. In turn, the crosslinks holding the gel network are eliminated and therefore the sample is converted to a sol. Our vesicle-gel thus serves as a photorheological (PR) fluid with

a 40 000-fold reduction in sample viscosity due to light. Because the gel-to-sol transition is accompanied by the disruption of vesicles, the above gel could also be envisioned as an injectable material for light-controlled delivery of drugs or other payloads.

Experimental section

Materials

p-(Octyloxyphenyl)phenyliodonium hexafluoro-antimonate (ODPI) was purchased from Gelest and sodium dodecylbenzenesulfonate (SDBS) was obtained from TCI. The nonionic surfactant Triton X100 was purchased from Sigma Aldrich. Sodium alginate (product number 4-00005) was purchased from Carbomer, Inc. and the molecular weight was specified by the manufacturer to be around 500 kDa. Disodium phosphate (Na_2HPO_4) was purchased from J. T. Baker and was used to make buffer solutions. All chemicals and materials were used as received without further purification. Ultrapure deionized (DI) water from a Millipore water purification system was used in preparing samples.

Surface tension measurements

The surface tension of ODPI solutions in 50 mM Na_2HPO_4 at different concentrations was measured by a Surface Tensiometer 21 (Fisher Scientific) using a platinum ring. Each solution was measured three times.

Sample preparation

Stock solutions of ODPI and SDBS were prepared separately by dissolving calculated amounts in 50 mM Na_2HPO_4 buffer at room temperature for 24 h. Vesicle solutions were prepared by mixing these stock solutions at the appropriate weight ratio. The mixture was stirred overnight using a magnetic stir bar. Sample vials were wrapped with aluminum foil to prevent exposure to visible light. Vesicle-gel samples were prepared by mixing appropriate amounts of a vesicle solution and an hm-alginate solution, followed by vortex mixing.

hm-Alginate synthesis

hm-Alginate was synthesized by amidation of sodium alginate as described previously.^{48–50} For the synthesis, the coupling agent *N*-(3-dimethylaminopropyl)-*N'*-ethylcarbodiimide hydrochloride (EDC) and the hydrophobic compound *n*-octylamine were purchased from Sigma Aldrich. 1.5 g of sodium alginate was dissolved in 75 mL of DI water and the solution was stirred overnight to obtain a homogeneous solution. To adjust the pH to around 3, 30 mL of 0.1 M HCl was added dropwise and the solution was further stirred for 2 h. 75 mL of methanol was then added dropwise and the solution was again stirred for 2 h. Next, a solution of 0.4 g of the coupling agent EDC in 5 mL DI water was added dropwise. 1.37 g of *n*-octylamine (corresponding to 124 mol% of the repeating units of alginate) in 5 mL of methanol was then added slowly and the mixture was stirred for 24 h under ambient conditions. During this stage, hm-alginate is generated by reaction (see Fig. S2a, ESI†). The product was precipitated by adding acetone and separated by

vacuum filtration. This purification step was repeated 3 times. The final hm-alginate was recovered by vacuum drying at room temperature. The hydrophobic modification degree was determined by ^1H NMR as described previously.⁴⁸ ^1H NMR spectra were taken on a Bruker AVANCE 500 MHz spectrometer. Spectra were referenced to the 3-trimethylsilylpropionic acid sodium salt- d_4 . The calculated degree of hydrophobic modification was 23 mol% (see Fig. S2c, ESI†).

Sample response before and after UV irradiation

Samples were irradiated with UV light from an Oriel 200 W mercury arc lamp. A dichroic beam turner with a mirror reflectance range of 280 to 400 nm was used to access the UV range of the emitted light. A filter for below 400 nm light was used to eliminate the undesired visible wavelengths. Samples (2.5 mL) were placed in a Petri dish of 60 mm diameter with a quartz cover, and irradiation was done for a specific duration under mild stirring with a magnetic stirring bar.

Dynamic light scattering (DLS)

Solutions were studied at 25 °C using a Photocor-FC instrument equipped with a 5 mW laser source at 633 nm. The scattering angle was 90°. The autocorrelation function was measured using a logarithmic correlator and this was analyzed by the Dynals software package to yield the average hydrodynamic radius.

Rheological studies

Steady and dynamic rheological experiments were performed on an AR2000 stress controlled rheometer (TA Instruments). Samples were run at 25 °C on a cone-and-plate geometry (40 mm diameter, 2° cone angle). Dynamic experiments were performed in the linear viscoelastic range of the respective samples.

Cryo-TEM

Specimens were prepared in a controlled environment vitrification system (CEVS) at 25 °C and 100% relative humidity.^{44,45} A drop of the sample was placed on a TEM grid covered with a perforated carbon film and blotted with a filter paper to form a thin film on the grid. The blotted sample was allowed to stand in the CEVS for 10–30 s to relax from the shear caused by blotting. The relaxed samples were then plunged into liquid ethane at its freezing temperature (−183 °C) to form vitrified specimens, which were then stored at −196 °C in liquid nitrogen until examination. Specimens were examined in a Tecnai T12 G2 TEM (FEI) at an accelerating voltage of 120 kV. Samples were placed in an Gatan cryo-specimen holder that maintained the samples below −175 °C. Imaging was done in the low-dose mode to minimize electron-beam radiation damage. Images were recorded digitally at nominal magnifications up to 46 000× on a cooled UltraScan 1000 Gatan camera, using the DigitalMicrograph.

Acknowledgements

This work was funded by grants from NSF and NIST. Undergraduate student Reza Hashemipour assisted with some of the experiments at UMD and his contributions are acknowledged. For the cryo-TEM work at the Technion, the financial support of the ISF and the Russell-Berrie Nanotechnology Institute (RBNI) are acknowledged.

References

- 1 J. Israelachvili, *Intermolecular and Surface Forces*, Academic Press, San Diego, 1991.
- 2 D. F. Evans and H. Wennerstrom, *The Colloidal Domain: Where Physics, Chemistry, Biology, and Technology Meet*, Wiley-VCH, New York, 2001.
- 3 D. D. Lasic, *Liposomes: From Physics to Applications*, Elsevier, Amsterdam, 1993.
- 4 A. Z. Wang, R. Langer and O. C. Farokhzad, Nanoparticle delivery of cancer drugs, *Annu. Rev. Med.*, 2012, **63**, 185–198.
- 5 V. P. Torchilin, Recent advances with liposomes as pharmaceutical carriers, *Nat. Rev. Drug Discovery*, 2005, **4**, 145–160.
- 6 M. Fathi, M. R. Mozafari and M. Mohebbi, Nanoencapsulation of food ingredients using lipid based delivery systems, *Trends Food Sci. Technol.*, 2012, **23**, 13–27.
- 7 M. R. Mozafari, C. Johnson, S. Hatziantoniou and C. Demetzos, Nanoliposomes and their applications in food nanotechnology, *J. Liposome Res.*, 2008, **18**, 309–327.
- 8 G. Betz, A. Aeppli, N. Menshutina and H. Leuenberger, *In vivo* comparison of various liposome formulations for cosmetic application, *Int. J. Pharm.*, 2005, **296**, 44–54.
- 9 H. Barani and M. Montazer, A review on applications of liposomes in textile processing, *J. Liposome Res.*, 2008, **18**, 249–262.
- 10 P. Shum, J. M. Kim and D. H. Thompson, Phototriggering of liposomal drug delivery systems, *Adv. Drug Delivery Rev.*, 2001, **53**, 273–284.
- 11 C. Alvarez-Lorenzo, L. Bromberg and A. Concheiro, Light-sensitive intelligent drug delivery systems, *Photochem. Photobiol.*, 2009, **85**, 848–860.
- 12 O. V. Gerasimov, J. A. Boomer, M. M. Qualls and D. H. Thompson, Cytosolic drug delivery using pH- and light-sensitive liposomes, *Adv. Drug Delivery Rev.*, 1999, **38**, 317–338.
- 13 D. Needham and M. W. Dewhirst, The development and testing of a new temperature-sensitive drug delivery system for the treatment of solid tumors, *Adv. Drug Delivery Rev.*, 2001, **53**, 285–305.
- 14 H. Karanth and R. S. R. Murthy, pH-sensitive liposomes – principle and application in cancer therapy, *J. Pharm. Pharmacol.*, 2007, **59**, 469–483.
- 15 A. Schroeder, J. Kost and Y. Barenholz, Ultrasound, liposomes, and drug delivery: principles for using ultrasound to control the release of drugs from liposomes, *Chem. Phys. Lipids*, 2009, **162**, 1–16.
- 16 A. Mueller, B. Bondurant and D. F. O'Brien, Visible-light-stimulated destabilization of PEG-liposomes, *Macromolecules*, 2000, **33**, 4799–4804.
- 17 T. Spratt, B. Bondurant and D. F. O'Brien, Rapid release of liposomal contents upon photoinitiated destabilization with UV exposure, *Biochim. Biophys. Acta, Biomembr.*, 2003, **1611**, 35–43.
- 18 R. H. Bisby, C. Mead and C. C. Morgan, Wavelength-programmed solute release from photosensitive liposomes, *Biochem. Biophys. Res. Commun.*, 2000, **276**, 169–173.
- 19 J. M. Kuiper and J. B. F. N. Engberts, H-aggregation of azobenzene-substituted amphiphiles in vesicular membranes, *Langmuir*, 2004, **20**, 1152–1160.
- 20 J. Zou, F. Tao and M. Jiang, Optical switching of self-assembly and disassembly of noncovalently connected amphiphiles, *Langmuir*, 2007, **23**, 12791–12794.
- 21 X. L. Liang, X. L. Yue, Z. F. Dai and J. Kikuchi, Photoresponsive liposomal nanohybrid cerasomes, *Chem. Commun.*, 2011, **47**, 4751–4753.
- 22 D. H. Thompson, O. V. Gerasimov, J. J. Wheeler, Y. J. Rui and V. C. Anderson, Triggerable plasmalogen liposomes: Improvement of system efficiency, *Biochim. Biophys. Acta, Biomembr.*, 1996, **1279**, 25–34.
- 23 B. Chandra, R. Subramaniam, S. Mallik and D. K. Srivastava, Formulation of photocleavable liposomes and the mechanism of their content release, *Org. Biomol. Chem.*, 2006, **4**, 1730–1740.
- 24 E. W. Kaler, A. K. Murthy, B. E. Rodriguez and J. A. N. Zasadzinski, Spontaneous vesicle formation in aqueous mixtures of single-tailed surfactants, *Science*, 1989, **245**, 1371–1374.
- 25 E. W. Kaler, K. L. Herrington, A. K. Murthy and J. A. N. Zasadzinski, Phase-Behavior and Structures of Mixtures of Anionic and Cationic Surfactants, *J. Phys. Chem.*, 1992, **96**, 6698–6707.
- 26 X. Wang, E. J. Danoff, N. A. Sinkov, J. H. Lee, S. R. Raghavan and D. S. English, Highly efficient capture and long-term encapsulation of dye by catanionic surfactant vesicles, *Langmuir*, 2006, **22**, 6461–6464.
- 27 E. J. Danoff, X. Wang, S. H. Tung, N. A. Sinkov, A. M. Kemme, S. R. Raghavan and D. S. English, Surfactant vesicles for high-efficiency capture and separation of charged organic solutes, *Langmuir*, 2007, **23**, 8965–8971.
- 28 H. Sakai, A. Matsumura, S. Yokoyama, T. Saji and M. Abe, Photochemical switching of vesicle formation using an azobenzene-modified surfactant, *J. Phys. Chem. B*, 1999, **103**, 10737–10740.
- 29 F. P. Hubbard, G. Santonicola, E. W. Kaler and N. L. Abbott, Small-angle neutron scattering from mixtures of sodium dodecyl sulfate and a cationic, bolaform surfactant containing azobenzene, *Langmuir*, 2005, **21**, 6131–6136.
- 30 Y. C. Liu, A. L. M. Le Ny, J. Schmidt, Y. Talmon, B. F. Chmelka and C. T. Lee, Photo-assisted gene delivery using light-responsive catanionic vesicles, *Langmuir*, 2009, **25**, 5713–5724.
- 31 A. Diguët, M. Yanagisawa, Y. J. Liu, E. Brun, S. Abadie, S. Rudiuk and D. Baigl, UV-Induced bursting of cell-sized

- multicomponent lipid vesicles in a photosensitive surfactant solution, *J. Am. Chem. Soc.*, 2012, **134**, 4898–4904.
- 32 W. M. Horspool and F. Lenci, *CRC Handbook of Organic Photochemistry and Photobiology*, CRC Press, Boca Raton, 2nd edn, 2004.
 - 33 K. T. Ren, J. H. Malpert, H. Y. Gu, H. Y. Li and D. C. Neckers, Synthesis, properties and photolysis of new iodonium tetrakis(pentafluorophenyl)gallate photoinitiators and comparison with their indate and aluminate analogs, *Tetrahedron*, 2002, **58**, 5267–5273.
 - 34 J. V. Crivello and M. Sangermano, Visible and long-wavelength photoinitiated cationic polymerization, *J. Polym. Sci., Part A: Polym. Chem.*, 2001, **39**, 343–356.
 - 35 W. A. Green, *Industrial Photoinitiators: A Technical Guide*, CRC Press, Boca Raton, 2010.
 - 36 A. M. Ketner, R. Kumar, T. S. Davies, P. W. Elder and S. R. Raghavan, A simple class of photorheological fluids: Surfactant solutions with viscosity tunable by light, *J. Am. Chem. Soc.*, 2007, **129**, 1553–1559.
 - 37 H. Oh, A. M. Ketner, R. Heymann, E. Kesselman, D. Danino, D. E. Falvey and S. R. Raghavan, A simple route to fluids with photo-switchable viscosities based on a reversible transition between vesicles and wormlike micelles, *Soft Matter*, 2013, **9**, 5025–5033.
 - 38 W. Meier, J. Hotz and S. GuntherAusborn, Vesicle and cell networks: Interconnecting cells by synthetic polymers, *Langmuir*, 1996, **12**, 5028–5032.
 - 39 F. E. Antunes, E. F. Marques, R. Gomes, K. Thuresson, B. Lindman and M. G. Miguel, Network formation of catanionic vesicles and oppositely charged polyelectrolytes. Effect of polymer charge density and hydrophobic modification, *Langmuir*, 2004, **20**, 4647–4656.
 - 40 J. H. Lee, J. P. Gustin, T. H. Chen, G. F. Payne and S. R. Raghavan, Vesicle-biopolymer gels: Networks of surfactant vesicles connected by associating biopolymers, *Langmuir*, 2005, **21**, 26–33.
 - 41 J. H. Lee, H. Oh, U. Baxa, S. R. Raghavan and R. Blumenthal, Biopolymer-connected liposome networks as injectable biomaterials capable of sustained local drug delivery, *Biomacromolecules*, 2012, **13**, 3388–3394.
 - 42 D. Y. Yu, F. Huang and H. Xu, Determination of critical concentrations by synchronous fluorescence spectrometry, *Anal. Methods*, 2012, **4**, 47–49.
 - 43 T. S. Davies, A. M. Ketner and S. R. Raghavan, Self-assembly of surfactant vesicles that transform into viscoelastic wormlike micelles upon heating, *J. Am. Chem. Soc.*, 2006, **128**, 6669–6675.
 - 44 D. Danino, Cryo-TEM of soft molecular assemblies, *Curr. Opin. Colloid Interface Sci.*, 2012, **17**, 316–329.
 - 45 D. Danino, A. Bernheim-Groswasser and Y. Talmon, Digital cryogenic transmission electron microscopy: an advanced tool for direct imaging of complex fluids, *Colloids Surf., A*, 2001, **183**, 113–122.
 - 46 D. Danino, Y. Talmon and R. Zana, Vesicle-to-micelle transformation in systems containing dimeric surfactants, *J. Colloid Interface Sci.*, 1997, **185**, 84–93.
 - 47 R. G. Larson, *The Structure and Rheology of Complex Fluids*, Oxford University Press, New York, Oxford, 1999.
 - 48 H. T. Bu, A. L. Kjoniksen, K. D. Knudsen and B. Nystrom, Effects of surfactant and temperature on rheological and structural properties of semidilute aqueous solutions of unmodified and hydrophobically modified alginate, *Langmuir*, 2005, **21**, 10923–10930.
 - 49 C. Galant, A. L. Kjoniksen, G. T. M. Nguyen, K. D. Knudsen and B. Nystrom, Altering associations in aqueous solutions of a hydrophobically modified alginate in the presence of beta-cyclodextrin monomers, *J. Phys. Chem. B*, 2006, **110**, 190–195.
 - 50 S. Choudhary and S. R. Bhatia, Rheology and nanostructure of hydrophobically modified alginate (HMA) gels and solutions, *Carbohydr. Polym.*, 2012, **87**, 524–530.
 - 51 C. W. Macosko, *Rheology: Principles, Measurements, and Applications*, VCH, New York, 1994.
 - 52 S. G. Oh and D. O. Shah, Micellar lifetime – Its relevance to various technological processes, *J. Dispersion Sci. Technol.*, 1994, **15**, 297–316.

Supporting Information for:

Light-Induced Transformation of Vesicles to Micelles and Vesicle-Gels to Sols

Hyuntaek Oh, Vishal Javvaji, Nicholas A. Yaraghi, Ludmila Abezgauz, Dganit Danino, Srinivasa R. Raghavan*

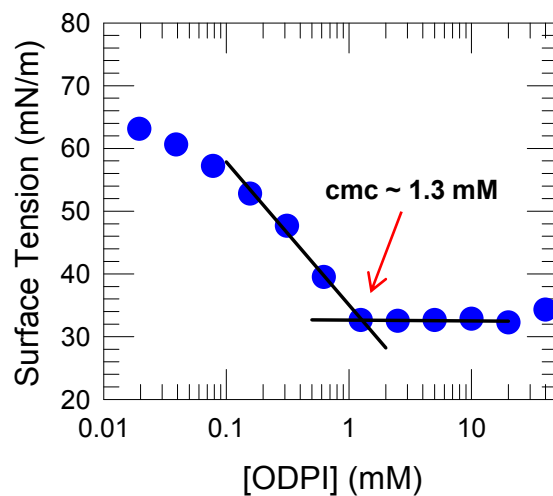
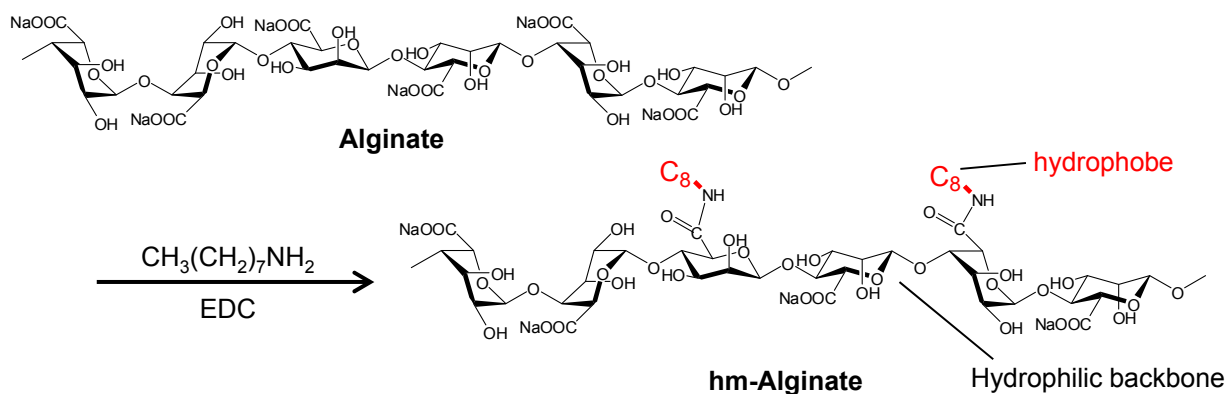
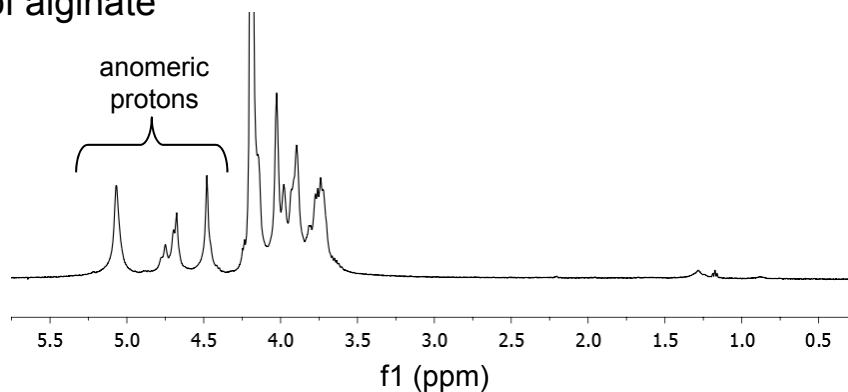


Figure S1. Surface tension values are plotted over the range of concentrations of ODPI in 50 mM phosphate buffer. The plot shows the typical behavior expected for surfactants, i.e., a drop in surface tension followed by a plateau. The CMC value obtained from the intersection point of the two regressed lines is 1.3 mM.

(a) hm-alginate synthesis



(b) NMR of alginate



(c) NMR of hm-alginate

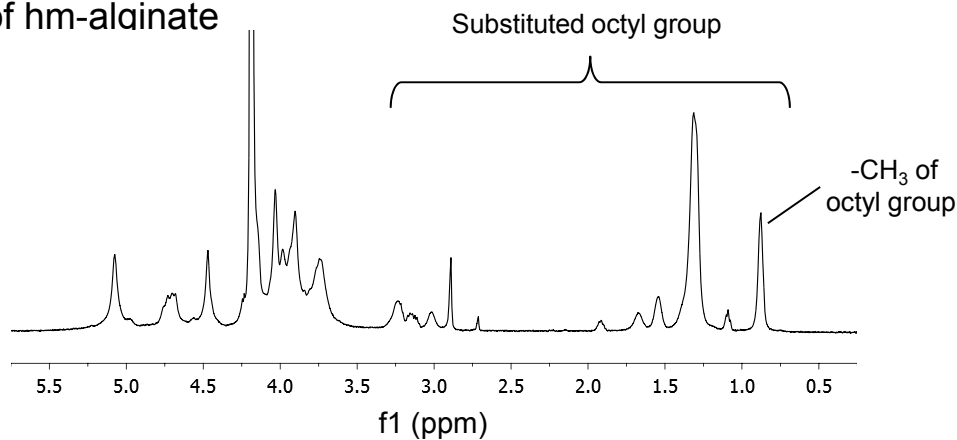


Figure S2. (a) Reaction scheme for synthesis of hm-alginate. This involves amidation of sodium alginate with n-octylamine using the coupling agent EDC. ¹H NMR spectra of alginate (b) and hm-alginate (c). From the peaks of anomeric protons, the G content of alginate was calculated to be 51.2%.¹ The ¹H NMR spectrum of hm-alginate shows additional peaks (0.8 ~ 3.3 ppm, 4.9 ppm) which indicate the successful modification of alginate with octyl groups. From the ratio of methyl protons to anomeric protons, the degree of modification was obtained to be 23%.²

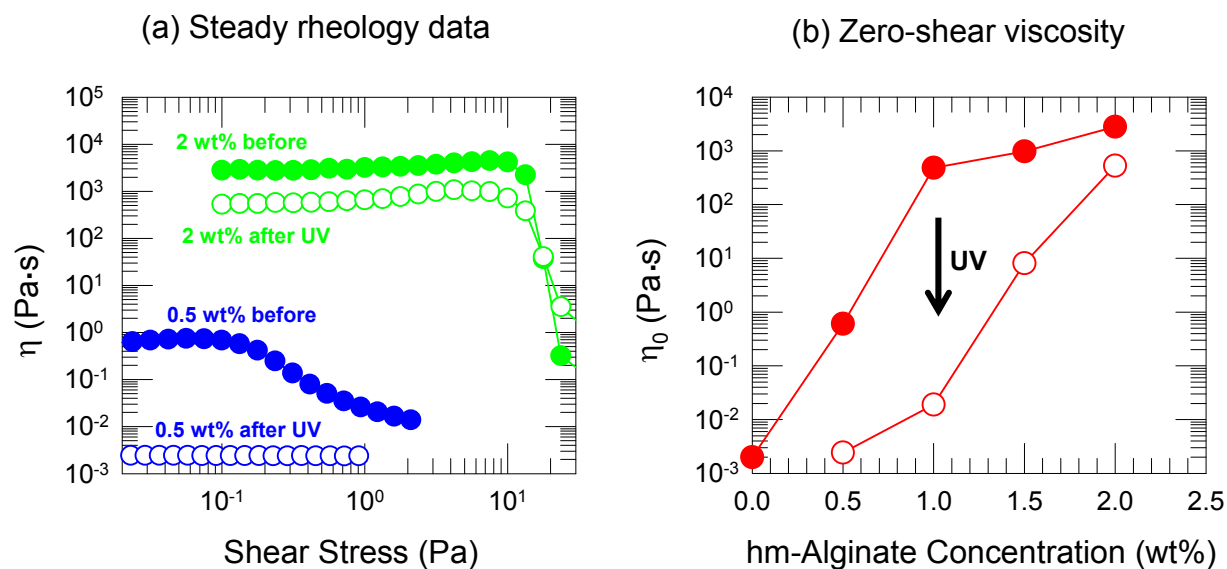


Figure S3. Rheology of vesicle gels before and after UV irradiation: Effect of altering the hm-alginate concentration at a constant ODPI/SDBS vesicle concentration of 2 wt%. (a) Representative steady-shear rheology data for samples before (closed circles) and after 45 min of UV irradiation (open circles): 2 wt% hm-alginate (green symbols); 0.5 wt% hm-alginate (blue symbols). (b) From the steady rheology data, the zero-shear viscosity η_0 is plotted against the hm-alginate concentration: before UV irradiation (closed red circles); after 45 min of UV irradiation (open red circles).

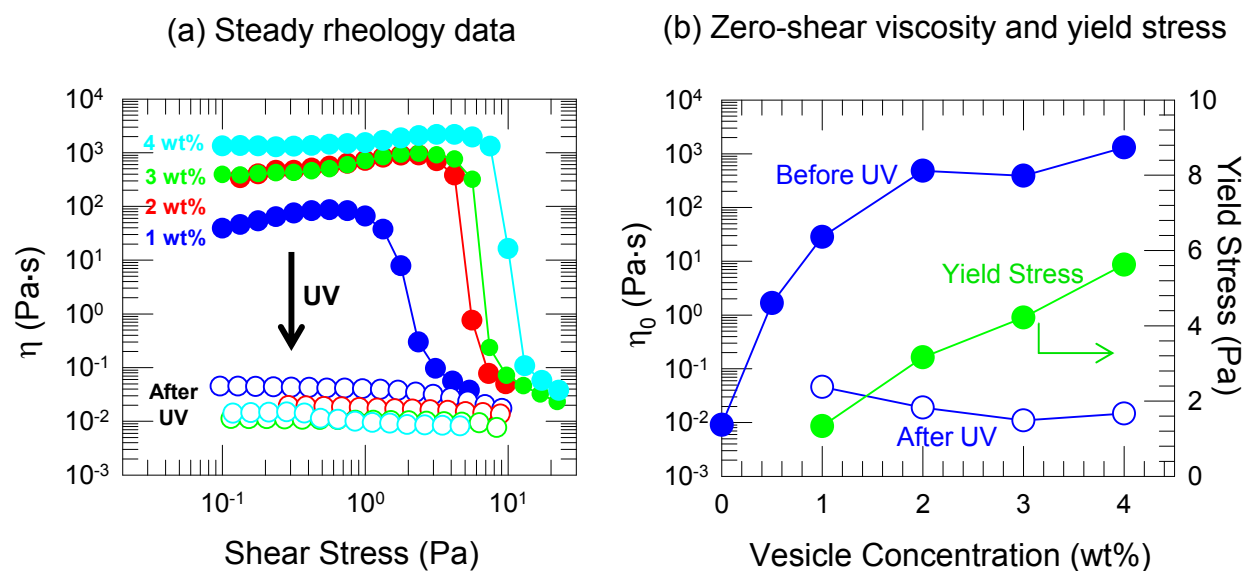


Figure S4. Rheology of vesicle gels before and after UV irradiation: Effect of altering the ODPI/SDBS vesicle concentration at a fixed hm-alginate concentration of 1 wt%. (a) Steady-shear rheology data for samples before (closed circles) and after 45 min of UV irradiation (open circles) for vesicle concentrations of 1 wt% (blue symbols), 2 wt% (red), 3 wt% (green) and 4 wt% (cyan). (b) From the steady-shear data, the zero-shear viscosity η_0 and the apparent yield stress (point of sharp drop in viscosity) are plotted against the vesicle concentration: η_0 before UV irradiation (closed blue circles); yield stress before UV irradiation (closed green circles); η_0 after 45 min of UV irradiation (open blue circles).

References

1. Pawar, S. N.; Edgar, K. J. "Alginate derivatization: A review of chemistry, properties and applications." *Biomaterials* **2012**, *33*, 3279-3305.
2. Galant, C.; Kjoniksen, A. L.; Nguyen, G. T. M.; Knudsen, K. D.; Nystrom, B. "Altering associations in aqueous solutions of a hydrophobically modified alginate in the presence of beta-cyclodextrin monomers." *J Phys Chem B* **2006**, *110*, 190-195.